BRAIN TUMOR SEGMENTATION USING REGION SPLIT AND MERGE TECHNIQUE

A DISSERTATION

Submitted in partial fulfilment of the requirements

for the award of degree of

MASTER OF TECHNOLOGY

in

COMPUTER SCIENCE AND ENGINEERING

by

AMALA THAMPI

COMPUTER SCIENCE AND ENGINEERING DEPARTMENT

INDIAN INSTITUTE OF TECHNOLOGY ROORKEE

ROORKEE - 247 667 (INDIA)

JUNE, 2016

CANDIDATE DECLARATION

I hereby declare that the work, which is being presented in the dissertation entitled "**Brain Tumor Segmentation using Region Split and Merge Technique**" towards the partial fulfilment of the requirement for the award of the degree of **Master of Technology** in **Computer Science and Engineering** submitted in the Department of Computer Science and Engineering, Indian Institute of Technology Roorkee, Roorkee, Uttarakhand (India) is an authentic record of my own work carried out during the period from July 2015 to June 2016, under the guidance of **Dr. R. Balasubramanian, Associate Professor**, Department of Computer Science and Engineering, IIT Roorkee.

The matter presented in this dissertation has not been submitted by me for the award of any other degree of this or any other Institute.

Date:

Place: Roorkee **(Amala Thampi)**

CERTIFICATE

This is to certify that the above statement made by my candidate is correct to the best of my knowledge and belief.

Date:

Place: Roorkee **(Dr. R. Balasubramanian)**

Associate Professor

Department of Computer Science and Engineering

IIT Roorkee

ACKNOWLEDGEMENTS

I would like to express my sincere gratitude to my guide Dr. R. Balasubramanian, Associate Professor, Department of Computer Science and Engineering, Indian Institute of Technology Roorkee, for providing me the opportunity to work on this topic as well as the help and support extended to me throughout the period of my dissertation.

I am extremely grateful to my parents who motivated me along this period and for the sacrifices they bore so that I could complete my dissertation successfully. I also thank my sister and my friends who supported me with their kind and encouraging words.

I also thank each and every person who helped me along, in one way or another, to complete my work. Finally, I thank God Almighty, without whose mercy, my efforts would not have become fruitful.

ABSTRACT

Brain tumor segmentation involves detecting the presence of tumor in the available brain scan image which is obtained from any neuroimaging machine. The main goal of any tumor segmentation algorithm is to automatically segment the tumor tissues, in whole or components (tumor core and edema), with maximum accuracy despite the nature of the tumor present. This involves studying the differences between normal brain tissue in various imaging modalities and choosing the most effective modality followed by applying a suitable algorithm to segment the tumor. The diagnostic machines used these days provide complete 3-dimensional data of the subject's brain. Hence a 3-dimensional algorithm is more suitable and effective in detecting the tumor tissues. The proposed algorithm combines the concepts of region split & merge and co-occurrence matrix to segment the tumor from the FLAIR modality slices. It also uses region growing method to further improve the result obtained in the first phase. The implementation involves the use of BRATS 2014 dataset. This is an automatic method which detects the tumor of various shapes, sizes and locations with a considerably high accuracy. The dice coefficient value to evaluate the test cases has an average value of 0.89 in case of High Grade Tumors and 0.85 in case of Low Grade Tumors.

TABLE OF CONTENTS

LIST OF FIGURES

LIST OF TABLES

ABBREVIATIONS

MRI……..Magnetic Resonance Imaging

HGG……..High Grade Glioma

LGG……...Low Grade Glioma

CT……...Computed Tomography

FLAIR……. Fluid-Attenuated Inversion-Recovery

PET……Positron Emission Tomography

FCM……Fuzzy C-Means

CNN……Convolutional Neural Network

2-D……2-Dimensional

3-D……3-Dimensional

CHAPTER 1

INTRODUCTION

Tumor segmentation has been a widely researched topic over the past decade. According to the studies of Cancer Research UK, 1 out of every 2 people is prone to develop cancer at some point of their lives. Growing number of cancer patients, along with the critical nature of illness have pushed the medical field to come up with fast and efficient methods to detect the presence of tumor cells.

Amongst the various cancer types, brain tumor is considered the most life-threatening, since the survival rate is considerably low compared to the other cancer types. The prognosis depends highly on the stage of the illness; hence it is necessary to diagnose the tumor at the earliest. Treatment for tumor varies with the stage at which the tumor is discovered. Early stage detection leads to the tumor removal by surgery or similar treatment methods whereas later stage requires chemotherapy in addition to the removal of tumor in order to prevent the tumor cells from growing or spreading to further sites.

Tumor segmentation involves processing the image, detecting the tumor if present, segmenting the entire tumor portion and extracting the area of interest. Additionally, more processing can be done to classify the tumor into edema(swelling caused by the tumor) and necrotic core, which helps better with the prognosis. The result of the segmentation must be more accurate since the prognosis depends on the size and location of the tumor.

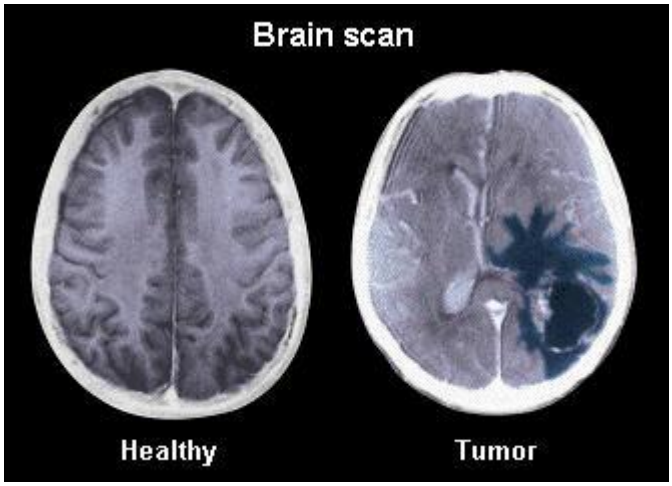

Fig. 1.1[36]: MRI scan image of brain tumor

Diagnosis can be conducted using methods like X-Ray, Ultrasonography, Magneto Encephalo Graphy (MEG), Magnetic Resonance Imaging (MRI), Computed Tomography (CT), Single-Photon Emission Computed Tomography (SPECT) Positron Emission Tomography (PET), etc. These imaging modalities provide a detailed report on the brain tumor. MRI-based tumor segmentation studies are getting more attention recently due to its non-invasive method of obtaining the images. The tumor can be detected and extracted by analysing these X-Ray images. Several methods have been used in the past to segment the tumor manually or automatically. Manual detection can delay the diagnosis as well as lead to wrong diagnosis from human calculation error. Automatic brain tumor segmentation is highly preferred so as to obtain error free results rapidly. There are many challenges in accurately segmenting the tumor from the MR Image such as varying sizes and shapes of tumor. Sometimes the tumor appears with edema which causes it to change its intensity.

The report has been divided into different section as follows: Chapter 2 contains details regarding brain tumor, its treatment options and various mechanisms used for the same. Chapter 3 is a summary regarding the motivation to research the topic of brain tumor detection and the nature of research work presently going on. Chapter 4 gives a detailed explanation regarding the working of the proposed algorithm, which includes the segmentation and extraction of tumor. Chapter 5 explains the refinement procedure of the extracted tumor tissues. Chapter 6 discusses the results of the algorithm on the test cases. Chapter 7 concludes the report along with the future work possible in this area. Chapter 8 gives the list of publications referred.

CHAPTER 2

BRAIN TUMOR

The tumor that originates in the spine or brain is known as brain tumor[4]. Around 80% of the malignant brain tumors falls under a particular type known as glioma. Symptoms may include problem with vision, headaches, vomiting, seizures and mental changes. In the worst case, it may lead to loss of consciousness. Gliomas can be further classified into different categories based on the cell type, grade of tumor and the location. Two main types of cancer are malignant tumor and benign tumor. Benign tumors do not have the ability to invade the adjacent tissues and are less aggressive. Hence they are non-carcinogenic. But they can be life-threatening at times, if they develop into malignant tumors through a process known as tumor progression. Common examples of benign tumors are moles or fibroids.

Malignant tumor involves abnormal cell growth that can spread to other locations of the body from the originating location. Symptoms of malignant tumor include lump, abnormal bleeding, prolonged cough, and unexplained loss of weight. There are over 100 known types of cancer depending on the originating site. Tobacco use, alcohol consumption, lack of physical activities, food and lifestyle etc. are some of the known causes of cancer. It can also be caused due to exposure to radiation, environmental pollutants and infections in certain cases.

Symptoms of brain tumor primarily depend on the location of tumor and its size. Primary brain tumors are the ones that originate inside the brain whereas secondary brain tumors are the ones that originated at some other point and eventually spread to the brain. Symptomsof both kind of tumors can be divided into three main categories:

- Increased intracranial pressure : Large tumors with edema result in elevated pressure which translates into headaches, nausea, vomiting, comatose, dilation of the pupil , papilledema.
- Dysfunction: depending on location of the growth and the consequent damage, neurologic symptoms may occur, such as intellectual and behavioural impairment including dizziness. diminished judgment, lack of perception, loss of memory, visual field impairment, spatial coordination disorders, dizziness, emotional or personality changes, facial paralysis, hypoesthesia, hemiparesis, ataxia, aphasia, weakened hearing, impaired sense of smell, double vision.

- Irritation: abnormal fatigue, weariness, tremors and absences, epileptic seizures.

2.1. WORLD HEALTH ORGANIZATION GRADING SYSTEM

Glioma is a term used to generally describe the tumor that arises from the supporting tissues of brain. An important classifying factor, is the tumor grades[5], which is a measure of the cell development stage and indicates how much the tumor has advanced. It is mostly applied to malignant tumors, and in some cases, benign tumors. There are various grading schemes[6] adopted, such as four-tier grading(low grade, intermediate grade, high grade, anaplastic), three-tier grading(low grade, intermediate grade, high grade) and two-tier grading scheme(low grade, high grade).

- Grade I [Low-Grade Glioma][7]- They look more like normal cells. They do not spread to other parts outside the brain, but grows locally into normal brain tissues. This can disrupt contact between normal brain cells and can become a source of pressure on the nearby brain, thus restricting the brain from expanding as it is confined in the skull. They tend to exhibit benign tendencies and has a more optimistic prognosis. But they have a uniform rate of repetition and increase in severity over the time. Hence they are categorized as malignant. Based on the appearance of the tumor, low-grade glioma is further categorised.
    - Low-grade astrocytoma: affects astrocytes, a type of glial cell
    - Low-grade oligodendroglioma: affects glial cells known as oligodendrocytes
    - Mixed glioma: includes both astrocytes and oligodendrocytes
- Grade II — Abnormal cells grow and spread more slowly. They may spread into nearby tissue and there are chances of recurrence. They may develop into high grade tumor.
- Grade III — The cells look very different from normal cells and can be distinguished under a microscope. They grow and spread quicker than grade I and II tumor cells. They are likely to spread into nearby tissue.
- Grade IV [High-Grade Glioma] - They appear different from normal cells under microscope and grow rapidly and are considered malignant and have a worse prognosis. Also known as Primary Brain Tumor.

Treatment options[8] include individual or combination of surgery, chemotherapy, radiotherapy and other palliative procedures.

- Surgery: partial or complete removal of maximum amount of tumor cells possible. Most opted surgical procedure is resection via craniotomy. Most cases of meningioma, except for some tumors detected at the base of the skull, can be successfully operated and removed.
- Radiotherapy: This is the most commonly adapted option for brain tumors; the tumor is illuminated with X-rays, beta or gamma rays. It is a method that uses computerized estimations to concentrate the radiation at the location of the tumor while reducing the dose to the surrounding brain, thus preventing any harm to the normal brain cells. It is the commonly used option for secondary brain tumors. The quantity of radiotherapy is determined by the size of the brain affected by cancer. Radiosurgery may be prescribed along with other treatments, or it may characterize the primary treatment method for some tumors.
- Chemotherapy: Although a treatment procedure for cancer, it is rarely used to treat brain tumors as the brain-blood boundary prevents the medicines from reaching the tumor cells. Chemotherapy prevents the growth and division of both normal and cancer cells in the body. Thus there are significant side effects suffered by patients availing chemotherapy such as nausea, hair loss, fatigue etc. Patients undergoing chemotherapy are provided with medicines designed to destroy tumor cells. The decision to prescribe chemotherapy to a brain tumor patient is determined by the patient's type of tumor, overall health and severity of the cancer. It is mostly provided for children. The toxicity and the side effects of the drugs, makes it the least preferred treatment option for brain tumor.

2.2 NEUROIMAGING

Neuroimaging[9] involves the various techniques used to image the structure and function of nervous system. It allows the physician to observe the neuroactivities inside the brain, the area affected by the tumor and helps them to administer the proper treatment based on the nature of tumor. Although there are a number of imaging techniques available, the most common brain imaging techniques are Computed axial Tomography Scan(CT/CAT Scan), Magnetic Resonance Imaging(MRI) and Positron Emission Tomography(PET), since they are non-invasive techniques that provide more accurate results.

Since different slices or segments of the scanned area are produced using these methods, they can be viewed in different planes. Three-dimensional planes used in anatomical structures consist of sagittal, axial and coronal view.

- Sagittal plane – anatomical plane that splits the body into left and right halves. Equivalent to the Y-Z plane.
- Axial plane – the horizontal or transverse plane that partitions the body into upper half and lower half. Equivalent to the X-Z plane.
- Coronal plane – frontal plane that divides the body into front and back halves. Equivalent to the X-Y plane.

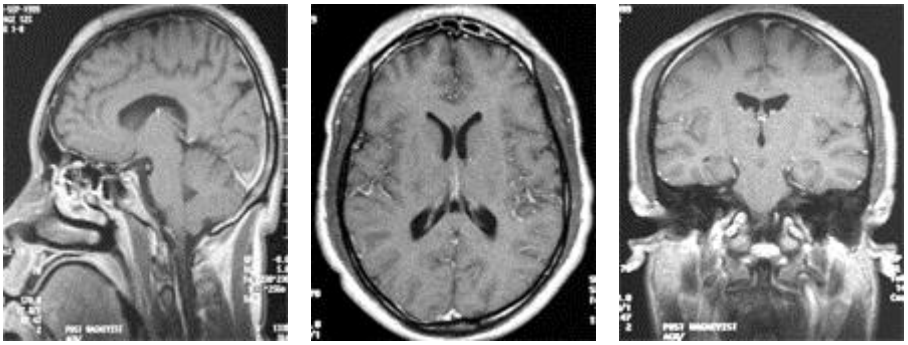

Sagittal View Axial View Coronal View

Fig. 2.1[37]: Different anatomical planes

2.2.1. Computed Axial Tomography

Tomography is derived from the Greek phrase ‘tomos’ meaning slices and ‘graphe’ meaning drawing. CT scanning[10] is based on the intake of x-rays by the body tissues, like X-Ray imaging technique. It differs from the conventional imaging technique in the sense it provides a type of imaging known as cross-sectional imaging. That is, it provides slices or cross-sectional images of the body part that is imaged.

CT Scanning works as follows: The machine consists of a motorized table on which the patient moves through the circular region used to image the body tissues. As the patient passes through the machine, a circular beam of x rays are passed which rotates around the patient. The thickness of the X-ray source varies from 1 millimeter to 10 millimeters. The patient may be administered an injection of a contrast material to increase the visualization of the irradiated part. An X-Ray snapshot consists of a particular angle or position of X-ray beam. Different snapshots are obtained from all the angles during a rotation. The various snapshots obtained are collected and reconstructed into a cross-sectional image of the required tissue.

Benefits:-

- Painless and quick method
- Diagnose a wider range of body tissues and medical conditions such as cancer, strokes etc.
- Avoids the need of surgery

Drawbacks:-

- Slight risk of cancer due to being exposed to ionising radiation (X-rays), especially in the case of children; also involves a higher dose of radiation compared to other methods
- The contrast material used can be harmful as it causes kidney-related diseases; non-suitable for pregnant women and children

2.2.2. Magnetic Resonance Imaging

Magnetic Resonance Imaging(MRI)[11] is a non-invasive method that produces three dimensional structured anatomical images for clinical purposes. It is based on technology that excites and aligns the protons found in the water that living tissues compose of with the strong magnetic field produced. It uses magnetic and radio waves to diagnose the medical condition of the patient.

MRI machine consists of a circular opening like that of CT Scanner. It uses superconducting magnets[h], which create a strong magnetic field up to 2 tesla. The human body is made up of large quantity of water and fat, and hence contain Hydrogen atom. Under normal conditions, these atoms are spinning randomly. When the patient enters the machine, the strong magnetic field produced forces the protons contained in the Hydrogen atoms line up in the direction of magnetic field. Since the magnetic field is applied at the center, it makes the protons in the region upward to point to the head and the region downward to point to the feet. Thus most of the protons cancel each other. The machine also applies radio frequency pulse, which is focused at the area of interest. It causes the uncanceled protons in that area to absorb the energy and spin in a direction, with a particular frequency known as Larmour frequency. When the radio frequency is switched off, the protons align back into their normal position causing them to release energy which is absorbed by the magnetic coil and this is sent to the computer in digital form.

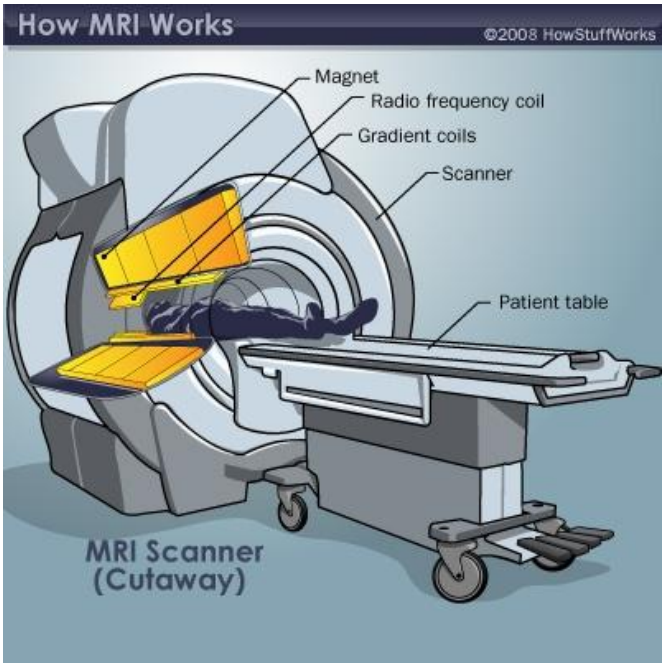

Fig. 2.2[11]: MRI machine

There are various MRI modalities based on the type of pulse sequence used in the imaging process. The basic goal of the different MR image channels is image contrast. It is influenced by different factors such as pulse sequence, echo time(TE), relaxation time(TR) etc. Based on the values of the above mentioned parameters, the following types of MR images are available:

- **T1**, or T1-weighted MRI: image contrast is based prominently on the T1 relaxation time of tissue, which is defined as the time when 63% of the longitudinal magnetization has restored. It is measured using a time constant called T1 usually in units of milliseconds. In this type, tissue with short T1 relaxation time appears brighter. Low grade tumor may not be enhanced in T1-modality.
- **T2**, or T2-weighted MRI: image contrast depends predominantly on the T2 relaxation time of tissue; T2 relaxation is defined as the time when 63% of the transverse magnetization has decomposed. It is measured using a time constant called T2 in units of milliseconds. In this case, tissue with long T2 relaxation time appears brighter compared to others. In T2 modality, tumor and edema detection is more efficient.

- **T1 Contrast Enhanced** MRI: MRI modality obtained after administering a contrast agent to T1-weighted MRI. Majority of tumors show signal enhancement in this MR image.

- **FLAIR**: also known as Fluid-Attenuated Inversion-Recovery MRI; This is considered as T2-weighted MRI without the presence of cerebrospinal fluid (CSF). FLAIR modality removes the fluid from the MRI which allows for a better detection of small lesions.

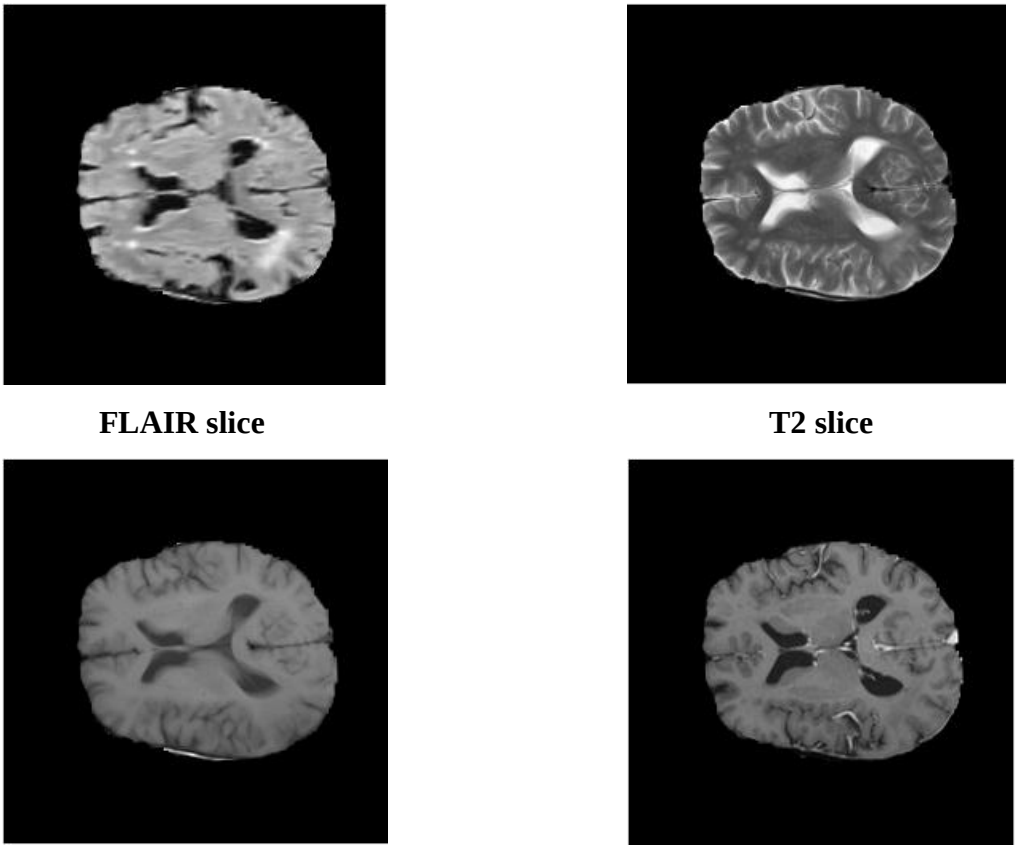

FLAIR slice **T2 slice**

T1 slice **T1 Contrast Enhanced slice**

Fig. 2.3: Various MRI modalities

The following are the advantages of using MRI scanning method:

- Non-invasive and painless method.
- They do not use the ionizing radiation of x-rays unlike CT scan and hence is safe.
- Contrasting agent used has less chance of producing an allergic reaction.

The disadvantages of MRI Scanning are less significant:

- Expensive method.

- Creates a loud noise during application.
- May not be suitable for claustrophobic people.

2.2.3. Positron Emission Tomography

It is an imaging technique used to observe the metabolic activities in the body at the cellular level. Gamma rays are introduced into the patient's body using a tracer. These emissions are then captured by an imaging device and a three-dimensional structure of the body part is reconstructed.

Although PET scanning is commonly used for tumor detection[12], it is also used in treating dementia and other neurological disorders, cardiac treatment and to evaluate brain trauma.

Since PET Scan detects the metabolic activities at the cellular level, it is more accurate compared to the other methods. It can be used to differentiate between malignant and benign tumor. The chance of getting an infection from this method is almost nil. On the downside, this procedure is considerably expensive.

CHAPTER 3

LITERATURE REVIEW

3.1. MOTIVATION

Medical Imaging is a field that requires high precision techniques that are also time efficient, since the clinical results play a huge role in the diagnosis and further treatment of the patient. A slight error may lead to entirely different diagnosis that may endanger the life of the patient. Hence this is an actively researched area. Brain tumor segmentation, in particular, has gained attention due to the critical nature of the issue. Inability to identify the situation at an early stage increases the mortality rate. Many a times the tumor is not visible to the naked eye due to its varying size, shape, location etc. So manual detection may not always lead to correct diagnosis. Automatic and semi-automatic detection techniques also have their share of disadvantages as most of the techniques developed have been tested only on a limited set of test data, and fail to identify the tumor position correctly on a wide range of dataset. Hence it is necessary to develop a technique that is accurate, less time-consuming and provides correct result for different kinds of data sets.

3.2. CURRENT STATE OF RESEARCH

Existing algorithms can be primarily classified into two categories: region-based and boundary based segmentation. They cover a number of methods like Bayesian Classifier, Fuzzy C-Means clustering, Neural Networks, Kernel Sparse representation, Expectation Maximization etc.

A knowledge-based automatic segmentation using outlier detection was proposed by Prastawa et al.[1] The abnormal regions in the brain MRI were detected based on a registered brain map as a template for healthy brains. Clustering based on intensity classified the tissues into different classes of normal and abnormal (tumor-affected) regions. This method fails if the brain MRI is not sampled correctly with the given brain atlas. Corso et al.[2] devised a Bayesian classification method which results in a model-aware multi-level segmentation by weighted aggregation algorithm, that can be applied to detect both tumor and edema in multichannel MR images. This model uses only local level statistics for its segmentation and does not take global context into account. Thiagarajan et al.[3] developed a low-complexity

segmentation approach in which kernel K-lines clustering is employed to create kernel dictionaries and use the kernel sparse codes to classify each pixel into normal and tumor classes. It was tested only for 15 data images.

Shen et al.[13] proposed Fuzzy C-Means (FCM) approach and its variations to segment the brain tumor. The MR image is segmented into normal and abnormal brain tissues using both traditional FCM and improved FCM. The modified method was found to perform better in the presence of noise. Havaei et al[14] proposed a Convolutional Neural Network(CNN) architecture that employs both local and global contextual information to segment the tumor. It also includes a 2-phase training to include various test cases of tumor sizes, shapes and intensities. This method has been specifically developed for glioblastoma tumor types. It also works on the individual 2-D slices of the three-dimensional dataset. Dvorak et al.[15] uses a local structure prediction method based on Convolutional Neural Network, where it takes an approach of localized structure through label path dictionaries, instead of using the voxel relationship and improve the performance of the prediction results using CNN.

Moon et al.[16] introduced Segmentation using Expectation Maximization method which alters a probabilistic brain atlas with the subject's information regarding tumor obtained from subtraction of pre- and post-contrast MRI. Xie et al.[17] proposed a semi-automated hybrid level set algorithm for segmentation which uses both boundary and region statistics. Region information acts as generation force, whereas barrier information works as the stopping criteria with a substantial accuracy. Cuadra et al.[18] devised a tumor segmentation method that makes use of a brain template. This involves 3 steps starting with the registration of the patients brain MRI with the brain atlas, growing the tumor radially from a seed point and deforming the seeded atlas.

Taylor et al.[19] presented a Map-Reduce enabled Hidden Markov method which is a supervised learning method for tumor segmentation. In the training phase, for each input voxel, a feature vector is extracted. The algorithm incrementally updates the training data set which is then used for feature extraction during testing. It has a high throughput, but the accuracy of the method is comparatively less. Meier et al.[20] proposed a generative-discriminative hybrid model which generates initial probabilities, that are later used to improve the classification and spatial regularization. They achieve an accuracy of 80% for complete tumor segmentation. Bakas et al.[21] introduced a 3-dimensional segmentation algorithm using hybrid generative-discriminative method. Initially, it uses a generalized

expectation-maximization method to segment the image into tumor and normal brain tissues. Later a probabilistic Bayesian model is used to finish the segmentation on the basis of patient-specific statistical values.

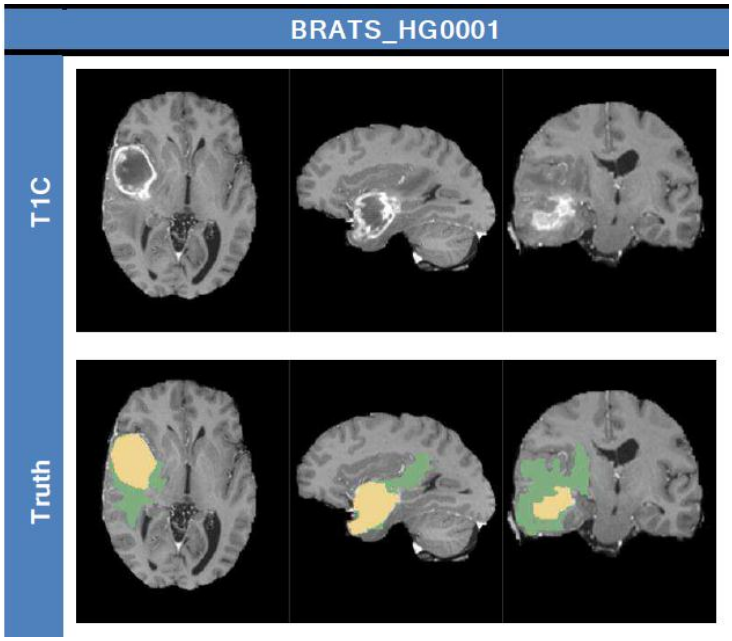

Fig. 3. 1[15]: Tumor segmentation using Hidden Markov Model

3.2.1. Drawbacks of existing algorithms:-

- Assumes symmetrical shape for brain – The algorithms[10,16] that use spatial brain atlas for the segmentation of brain assumes that the brain is symmetrically shaped. This class of algorithms fails especially when the tumor causes deformation of the brain.
- Implementation on 2-D slices - The proposed algorithm is implemented individually on the 2-D[13,14] slices rather than the three-dimensional data. This increases the time complexity of the algorithm and reduces the accuracy.
- Semi-automated algorithms – These approaches[17,18] require human intervention to some extent and also the accuracy depends on the initial parameters chosen.
- High Time Complexity – Time complexity is high for many algorithms based on the input size, algorithm, platform used etc.

CHAPTER 4

BRAIN TUMOR SEGMENTATION

4.1. PROBLEM STATEMENT

Given a 3-D MR image of brain, detect the presence of whole tumor. Using a fully automated algorithm, segment and extract the tumor region for further clinical analysis, irrespective of its size, shape or any other attributes.

4.2. PROCESS OVERVIEW

The process involves a sequence of steps such as pre-processing, initial segmentation, tumor extraction and refinement of result. Pre-processing is further defined into various processes such as skull-stripping, normalization and denoising. After the pre-processing step, initial segmentation is carried out by applying region split & merge along with the properties of co-occurrence matrices. The segmented tumor is then extracted using connected component labeling algorithm. The extracted tumor is then refined using region growing method and hole-filling algorithm. Each of the processes have been explained in detail later.

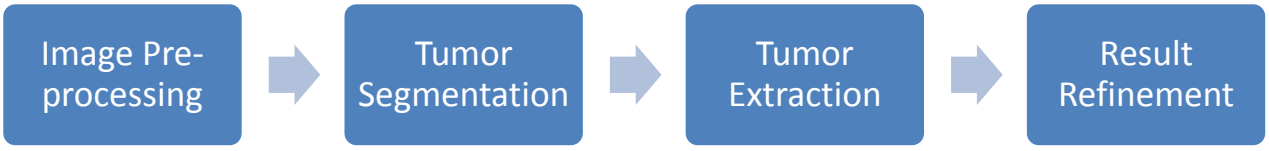

Fig. 4.1: System Overflow

4.3. IMAGE PRE-PROCESSING

Image pre-processing is the set of operations applied to an image to enhance its interpretability and improve the accuracy of the subsequent image processing techniques. Pre-processing includes noise filtering, normalization, histogram equalization etc. This is a necessary step in any kind of image processing technique as it affects the result considerably. Presence of noise in an image reduces the accuracy of the result.

Skull stripping[22] or scalp editing is the process of removing the non-brain areas such as skull before normalizing the image. The non-brain tissues such as eye balls, skin, bones etc. act as deterrents in the automatic brain tumor segmentation. Thus skull-stripping enhances the robustness of the processing especially, in image registration since the clinically obtained structural images usually contain non-brain tissues whereas the registered image usually does not contain them. There are mainly 5 categories[23] of methods available currently: intensity-based, mathematical morphology-based, atlas-based, deformable surface-based and hybrid methods. The data set that we are working on is already provided after skull-stripping. Hence we are not going into more details regarding these techniques.

FLAIR & T2 modalities are the most preferred since the tumor appears brighter in these two images. FLAIR modality enhances the contrast by decreasing the intensity of Cerebro Spinal Fluid. Hence FLAIR modality is chosen from the dataset.

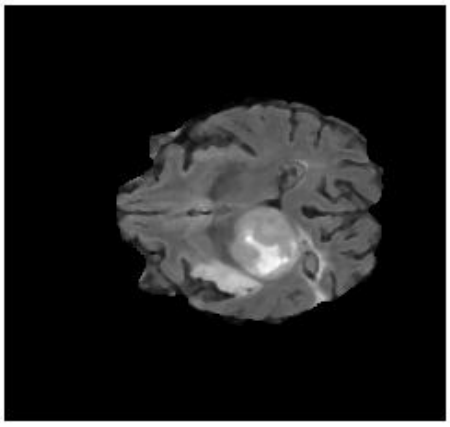

Fig. 4.2: Case HGG 404 FLAIR

The algorithm is run individually on a stack of 2-dimensional slices, which form the 3-dimensional MRI volume. The given input data has intensity values ranging from 0 to 1273. The images have been converted to grayscale type for usability. Hence the data has been normalized to the output range of 0-255, where 0 represents black and 255 represents white, as per the normalization equation given below:

$$v' = \frac{v-min}{v-max} * (new\_\max - new\_min) + new\_min \qquad (4.1)$$

where *v'* is the corresponding intensity of original intensity *v* in the new intensity range [*new_min,new_max*] and [*min,max*] is the original intensity range.

In order to remove the presence of noise signals in the input data, median filter is applied to the normalized FLAIR images where a window of 4 is used. If in a window of pixel values, there is a pixel value not representative of its surroundings, that is, its intensity value varies significantly from the rest of the pixel values, the pixel value is considered corrupted. The value is replaced by the median of all the pixel values sorted in ascending order.

FLAIR slice before pre-processing FLAIR slice after pre-processing

Fig. 4.3: Pre-processing of Input(Case HGG 10)

4.4. TUMOR SEGMENTATION

This is the most important step of the process that involves classifying the input MRI image into the insignificant background pixels, normal brain tissue and the tumor affected region. Various segmentation procedures are available in the literature. They can be primarily classified as thresholding, edge-based and region-based segmentation techniques. Here we employ a region-based classification method.

4.4.1. Region Split & Merge

Region split and merge[24] classifies an image into different classes based on homogeneity of pixels. The working of this technique is based on quadtrees. Each node of the tree can be split into 4 components, where the image is considered as the root of the tree. Hence, each node has 4 descendants. Each node is split into its descendants, based on the value of a predicate function.

The entire procedure consists of mainly 2 steps:

- Splitting: This step involves splitting a region into into 4 quadrants based on the predicate value
- Merging: When splitting is no more possible, start merging the adjacent regions that have the same predicate value.

Let R be the region under consideration, which is made up of its 4 quadrants R_1, R_2, R_3 and R_4. Let PREDICATE be a Boolean function whose output can be either True or False. If the value of the PREDICATE is False for any of the 4 quadrants, then the region R is split into the 4 quadrants. If the value of PREDICATE is True, then the region R is left as it is. This is the splitting procedure. In the merging procedure, if two adjacent regions R_i and R_j both satisfy the function PREDICATE, then they are merged together as they are considered part of the same class of pixels.

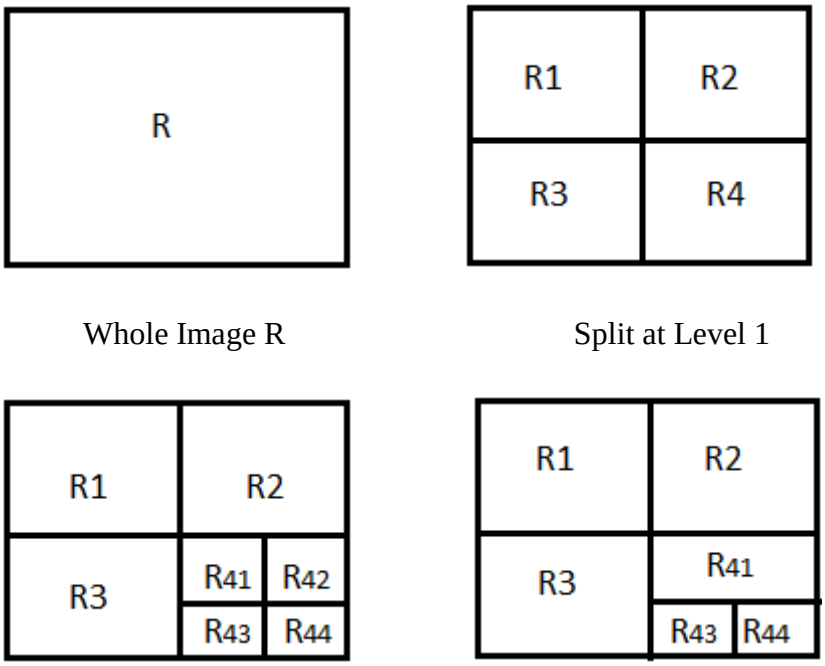

Whole Image R | Split at Level 1

Split at Level 2 | R after merging R_{41} and R_{42}

Fig. 4.4: Region Split & Merge Procedure

The minimum size of a node until which it can be split is provided to determine the extent of split and merge operation. It is usually taken as powers of 2. Hence the minimum size of a node is 1. Since the minimum dimension value of splitting can be adjusted, the resolution of

the segmentation can be varied accordingly. On the downside, it may lead to segmentation in the form of rectangular blocks as the splitting and merging is done in blocks of powers of 2.

4.4.2. Co-occurrence Matrix

Co-occurrence matrix[25] is a method used to analyse the texture of an image. Based on the texture of an image, we can identify the various regions of interest and the aspects in which they differ from one another. Co-occurrence matrices are usually defined for gray level images. Let I be an image with K gray levels. Then the co-occurrence matrix C is a matrix of order N in which the entry (*i* ,*j*) is defined as the number of occurrences of gray level value *i* adjacent to gray level *j* in I. The adjacency can be defined in terms of the direction of the gray values, ie., horizontal, vertical, left and right diagonal.

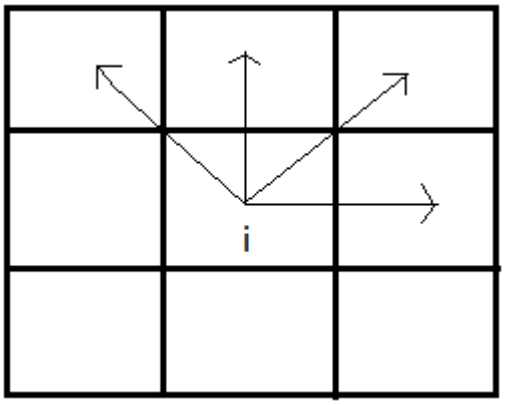

Fig. 4.5: Possible adjacent locations of j in co-occurrence with i

A number of attributes[26] can be calculated using co-occurrence matrix which gives an idea regarding the homogeneity of the image. For an image I, let *i* and *j* be any two adjacent locations and $p(i,j)$ be the cell value in the co-occurrence matrix J. μ_i, μ_i, σ_i and σ_j are the mean and standard deviations.

Table 4.1: Statistical values obtained from Co-occurrence Matrix

Attribute	Definition	Value
Contrast	Measures the contrast between two adjacent pixels over the entire image. Range = $[0,(N-1)^2]$ Value is 0 for a consistentt image.	$\sum_{i,j} \lvert i - j \rvert p(i, j)$
Correlation	Measure of the extent of correlation of two adjacent pixels over the whole image. Range = [-1 1]	$\sum_{i,j} \frac{(i - \mu_i)(j - \mu_j)\, p(i, j)}{\sigma_i \sigma_j}$
Energy	Sum of squared elements in the co-occurrence matrix Range = [0 1] Value is 1 for a constant image.	$\sum_{i,j} p(i, j)^2$
Homogeneity	Calculates the closeness amongst the elements in the co-occurrence matrix to the diagonal. Range = [0 1] Value is 1 for a diagonal GLCM	$\sum_{i,j} \frac{p(i, j)}{1 + \lvert i - j \rvert}$

In our procedure, Split and Merge algorithm is run individually on the 2-dimensional MRI slices. The minimum dimension until which the region is split, MINDIM, is set as 4. This is to avoid over-segmenting, in the case of MINDIM value 2, and under-segmenting, in case of MINDIM value 8. The image is padded with zeros until the size becomes a power of 2. The predicate function is run on the entire image, and based on the output value, it is split into its respective quadrants. The criteria set for splitting is given as follows:

$$flag = energy_R < 0.9 \;\&\; \bigcup_4^{i=1} mi < 165 \tag{4.2}$$

where $energy_R$ denotes the energy attribute of the region R obtained from calculating the co-occurrence matrix C, and m_i corresponds to the mean value of the intensities of quadrants R_1, R_2, R_3 and R_4.

Table 4.2: Intensity properties of tumor tissues

Case	Min. Intensity	Max. Intensity	Mean	Std. Deviation
HGG 1	40	236	142.06	8.39
HGG 2	67	172	139.29	8.86
HGG 10	120	190	150.96	8.35
HGG 198.1	33	233	156.80	9.77
HGG 368	61	211	151.79	10.76
HGG 412	69	237	168.18	9.45
HGG 444	87	225	158.94	10.24
LGG 8	53	176	138.81	8.75
LGG 130	107	155	141.78	5.35
LGG 298	14	250	146.54	10.74
LGG 428	96	225	174.92	10.01

Table 4.3: Intensity properties of brain tissues

Case	Min. Intensity	Max. Intensity	Mean	Std. Deviation
HGG 1	1	141	69.71	8.91
HGG 2	1	143	76.67	10.50
HGG 10	1	185	102.18	11.69
HGG 198.1	2	171	92.60	10.23
HGG 368	4	171	66.06	8.20
HGG 412	4	176	100.83	10.33
HGG 444	4	200	87.97	11.05
LGG 8	1	153	80.32	8.72
LGG 130	1	111	99.46	10.66
LGG 298	4	107	112.07	9.22
LGG 428	3	162	106.68	9.02

From the training set, it has been observed that, on an average, the tumor tissues have an intensity value in the range 165 – 255, whereas majority of the normal tissues have values in the range 1 - 175. Regions with high intensity values have high energy whereas those with low intensity values have low energy value. Hence a region is split if its energy value is low and if any of the quadrants has a mean value comparable to that of non-tumor tissue. The process is repeated until the condition is no longer satisfied or if the size of R becomes equal to MINDIM. After the splitting step is over, merging starts, where adjacent regions are combined if they have the same value for predicate function. When the merging process is over, the image is segmented into different regions based on homogeneity.

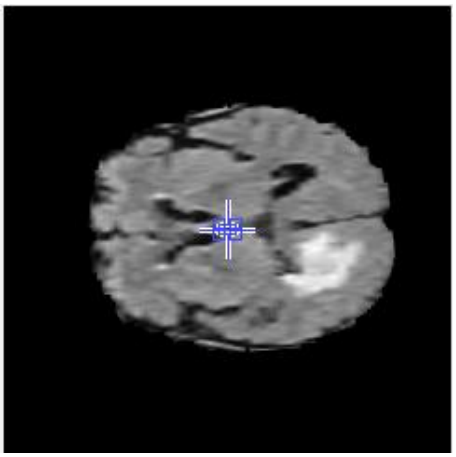

Case HGG 2 FLAIR

Case HGG 2 Segmented after Region Split & Merge

Fig. 4.6: Segmentation using Region Split & Merge

4.4.3. Pseudocode for tumor segmentation

I/P: FLAIR image I_{flair} & MINDIM = 4

O/P: Segmented image $I_{segment}$

SEGMENT(I_{flair}, MINDIM)

1) for S ← 1 to size ($I_{flair\ Z}$)
2) while (1)
3) R ← S;
4) (R_X , R_Y) ← size(R)
5) R_1 ← (1:R_X/2 , 1:R_Y/2) , R_2 ← (R_X/2 + 1: R_X/2, 1:R_Y/2) , R_3 = (1: R_X/2, R_Y/2 + 1:R_Y) , R_4 = (R_X/2 + 1: R_X, R_Y/2 + 1:R_Y)
6) m_i ← mean(R_i) ,$1 \leq i \leq 4$
7) GLCM ← co-occurrence_matrix(R)
8) (M , N) ← size(GLCM)
9) for i ← 1 to M
10) for j ← 1 to N
11) $energy_R = \sum_{i\,j} p(i,j)^2$
12) end for
13) end for
14) if $energy_R < 0.9$ & ($m_1 < 165 \mid m_2 < 165 \mid m_3 < 165 \mid m_4 < 165$)
15) flag ← 1
16) else
17) flag = 0
18) end if
19) if flag = 1 & size(R) > MINDIM
20) split R into R_1, R_2, R_3 and R_4

21) Continue the process for R_1, R_2, R_3 and R_4

22) else

23) break

24) end if

25) end while

26) end for

4.5. TUMOR EXTRACTION

The image obtained after running region split and merge consists of a number of segmented regions based on their intensity and texture. They can be called as a collection of connected components. The goal is to extract the tumor component from the set of components. For this, we apply connected components labelling algorithm.

After segmentation, the resultant slice has the voxels clustered into *C* categories. In some cases, some extraneous pixels are also classified into the tumor class due to its intensity similarity. Hence, the tumor region should be extracted from the slice. Connected Components algorithm is used for this purpose. Since the operation is done on a 2-D slice, 8 connected neighbors is used.

4.5.1. Connected Component Labeling Algorithm

Connected component labeling algorithm[27] works by scanning each of the pixel in the image. When it encounters a pixel whose intensity value is 1, it checks all of its 8 neighbors. If none of the neighbors have been already labelled, then a new identifying value is assigned to the pixel. If any pixel has already been labelled, then the present pixel is assigned the same label. If more than 1 neighboring pixels have been assigned different labels, then assign one of the labels to the current pixel and create equivalence between the two labels. After all the pixels have been scanned, all the equivalent pairs are sorted into a class and a unique label is assigned to all the values in the class, which is then updated in the image. The set of pixels with the same label form a component. The image will have *k* connected components, which are disjoint with each other.

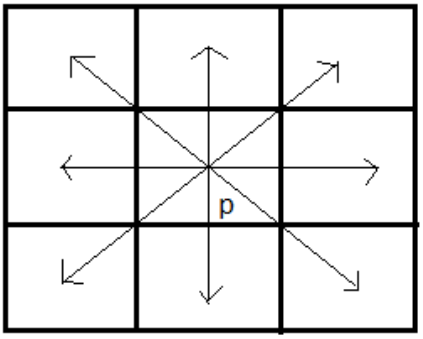

Fig. 4.7: 8-neighborhood of a pixel p

Generally, tumor has a convex shape, while the brain walls are highly irregular. The shape of an object can be analysed using a shape factor known as circularity[28]. It can be measured as follows:

$$\text{circularity} = (\text{perimeter})^2 / (4 * \text{pi} * \text{area}) \quad (4.3)^{[28]}$$

Perfectly spherical objects have circularity value = 1, and convex objects have a circularity value of 2. Objects that are mainly convex in nature except for a few irregularities, that is, a mix of convex and concave shape nature will have circularity value 3. Hence, in order to account for tumors that are both convex and slightly concave in nature, we set a threshold t = 3. Thus, we extract the components that have circularity < 3.

This method ensures that regions belonging to brain wall are rejected. Still, there can be some pixels that have been wrongly categorized into the tumor class. It usually happens if there is a large area of brain tissue that has intensities similar to the tumor region. Hence, we use the mean intensity value to extract the final tumor component. The component with the largest mean intensity value is chosen. Since the tumor class has intensity values higher than the normal brain tissues, its mean value will definitely be high. At the same time, if there is a larger area brain tissue component that was segmented by the split and merge algorithm, its overall mean value will be lesser since the area is greater, hence the number of pixels is also greater. Thus the tumor is extracted as follows:

$$Circularity < t \;\&\; max\,(mean_k),\ t = 3 \quad (4.4)$$

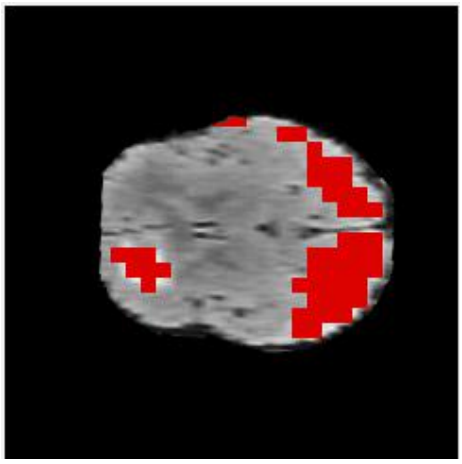

Case LGG 15:Tumor to be extracted relatively smaller in size

Fig. 4.8

4.5.2. Pseudocode for tumor extraction

I/P: Unlabelled Segmented Image from Region Split & Merge $I_{segment}$ where

$I_{segment}(x,y,z) = 1$, foreground pixel,

0, background pixel

O/P: Binary Image with extracted tumor I_{out}

EXTRACT($I_{segment}$)

```
1)   label_value ← 0
2)   for S ← 1 to I_segment(3)
3)    for i ← 1 to S(1)
4)      for j ← 1 to S(2)
5)        if  S(i,j) = 1 & S(i,j) is unlabelled
6)          if all 26 neighboring pixels are unlabelled
7)            label_value ← label_value+1
8)            S(i,j) ← label_value
9)          else if atleast 1 neighbor is labelled
10)           assign minimum(label_value) of all the neighbors to S(i,j)
11)         end if
```

12) end if

13) end for

14) end for

15) Generate equivalence class of all labels

16) for each labelled component k in S

17) if $\text{circularity}_k < 3$

18) calculate mean intensity value mean_k of k

19) end if

20) find component K where $\text{mean}_K = \text{maximum}(\text{mean}_k)$

21) end for

22) for each labelled component k where $k \neq K$

23) for each pixel S(i,j) in k

24) Set $S(i,j) \leftarrow 0$

25) end for

26) end for

27) end for

CHAPTER 5

RESULT REFINEMENT

Since region split and merge algorithm merges in powers of 2, the segmented region is usually rectangular in nature. This either leads to some parts of the tumor not being included or segmentation of extraneous pixels. Hence, the resultant image needs to be refined. Region growing algorithm is used for this purpose.

5.1. REGION GROWING TECHNIQUE

Region growing is another region-based segmentation technique. The process starts with the selection of seed point(s)[29]. These seed points are pixels that are guaranteed to be the part of the segmented region. After the selection of seed points, the next step is to grow the region from these points based on the intensity values of their neighboring pixels. If the neighboring pixels satisfy certain criteria, they are also added to the segmented image. Once again the algorithm is repeated for the neighboring pixels of the added pixel. The algorithm is repeated until no more pixels satisfy the criteria for region growing.

Region growing can be implemented by the selection of a single seed point or multiple seed points. While selection of a single seed point increases the execution time of the algorithm, selection of multiple seed points leads to increase in complexity of the algorithm. Selection of seed point(s) is the most important step in the algorithm as it affects the accuracy of segmentation. Many factors can be considered for the selection of seed point such as intensity value, location etc. This algorithm segments most of the images properly, but it may fail if the intensity values are closely similar throughout the image, such as the presence of noise in the form of shadows.

In our method, we employ the selection of a single seed to start the algorithm, since we already have completed initial segmentation. We choose the centroid point of the extracted region as the seed point. The centroid point or the center of mass is calculated as the center location of the region of interest. For a 2-dimensional body defined by a set X, the centroid is calculated as

$$\text{Centroid} = \frac{\int x \,.g(x)\, dx}{\int g(x)\, dx} \qquad (5.1)^{[30]}$$

where x is the value at that point and g is a function whose value is 1 inside X and 0 otherwise. Since we have chosen the centroid as the seed point, we assume that all its neighbors are also part of the segmented region. Hence we choose all of its 26 neighbors automatically without evaluating the membership criteria on each of them. We run a recurring function where in each round, for all the newly added pixels, the membership criteria is run on all of its 26 neighbors. All the neigboring pixels that satisfy the criteria are added to a queue, which becomes the input set for the next round. This continues until the queue has no elements to run the algorithm.

We calculate the mean and standard deviation values of the segmented region. For each neighboring pixel j of the current pixel i which is considered, if the intensity value of j is within a given range from the intensity value of i, it is added to the segmented region. The membership criteria to decide is given as follows:

$$S(j) \in [\ \mu_{cur} - a*\sigma_{cur}\ ,\ \mu_{cur} + a*\sigma_{cur}\ ] \qquad (5.2)^{[31]}$$

where S is the 2-D slice currently being processed, μ_{cur} is the current mean value of the region, σ_{cur} is the current standard deviation of the region and a is the scaling factor. After the membership criteria is executed for all the neigboring pixels of all the pixels in the queue, the new mean and standard deviation is calculated for the next round.

The scaling factor a is set based on the input data used. If the input data I belongs to the class of High Grade tumors, a takes values in the range [1.8 , 2]. For Low Grade tumors, this range varies slightly higher. Here the scaling factor a takes values in the range [2.2 , 2.8] with most of the cases working close to 2.8. This value was derived from the observations based on the training data.

$$1.8 \leq a \leq 2\ , \quad \text{if } I \in HGG \qquad (5.3)$$

$$2.3 \leq a \leq 2.8\ , \quad \text{if } I \in LGG$$

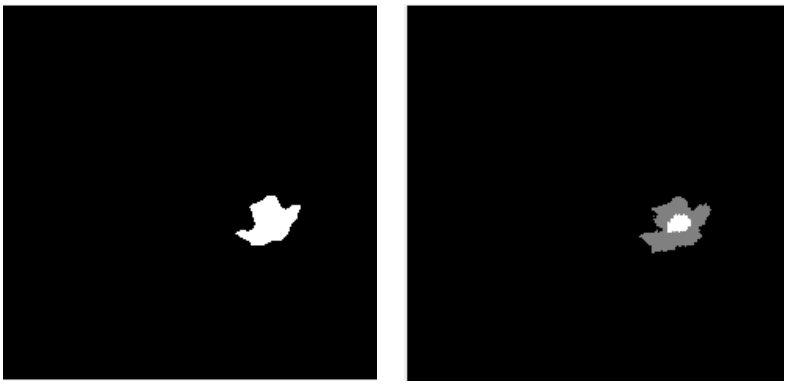

Case HGG 2 Refined result Case HGG 2 ground truth

Fig. 5.1: Result after applying Region Growing

5.1.1. Pseudocode for refinement using Region Growing

I/P: I_{out} with extracted tumor

O/P: Refined result I_{result}

REGION_GROW(I_{out})

1) for S ← 1 to $I_{out}(3)$
2) if extracted component $K \neq$ NIL
3) Centroid ← centroid(*K*)
4) S(Centroid) ← foreground
5) for i ← 1 to size(S),
6) if i ≠ Centroid
7) S(i) ← background
8) end if
9) end for
10) Q ← NULL
11) Add Centroid to Q
12) for all 26 neighbors $Neigh_{Centroid}$ of Centroid
13) $S(Neigh_{Centroid})$ ← foreground
14) Add $S(Neigh_{Centroid})$ to Q

15) end for

16) $\mu_{cur} \leftarrow$ mean(Q)

17) $\sigma_{cur} \leftarrow$ std(Q)

18) end if

19) flag ← 1

20) while (flag)

21) for i ← 1 to size(Q)

22) for each background neighbour j of i

23) if S(j) ϵ [μ - a*σ , μ + a*σ]

24) add j to Q

25) end if

26) end for

27) Q ← Q - i

28) end for

29) if Q ≠ NULL

30) $\mu_{cur} \leftarrow$ mean(Q)

31) $\sigma_{cur} \leftarrow$ std(Q)

32) else

33) flag ← 0

34) end if

35) end while

36) end for

37) end for

5.2. FILLING HOLES & GAPS

After refining the segmented image using region growing algorithm, certain cases of tumors may have unfilled holes and curves that are actually part of the tumor. Hence these holes need to be closed.

Fig. 5.2: Case HGG 444: extracted tumor with a hole

Before filling the holes, we need to trace the boundary of the region, so that the region is well-defined. A morphological reconstruction method known as imclearborder which is part of an Image Processing toolbox[32] of MATLAB, is used for this purpose. If a structure contains a region along the image boundary whose intensity value being closer to the surrounding non-border area, it is removed from the boundary region using this method. It uses a masking structure along with the image as input. The user can also decide the connectivity value of 4 or 8, based on the number of neighbors that need to be considered while filling the border areas. The mask image is set as zero everywhere, except for those pixels that belong to the border areas of the image. Once the connectivity parameter is decided, the neighbors along the connectivity of the boundary regions whose intensity is lighter than the surrounding region is cleared, or defined as 0.

The next step is to fill any gaps that are present in the image. Morphological closing is an operation that can be used to close the gaps in an image. Using a structural element, this method closes the gaps according to the shape taken by the structuring element. It is a sequence of two operations, dilation and erosion respectively, both of which uses the same structuring element. A structuring element is a binary n-dimensional array, which is true for all the locations that are part of the shape of the element and false for the rest of the locations. There are a number of structuring elements available such as line, disk, diamond, sphere, square etc. The user can specify the required dimensions as well as the alignment for each of the elements.

5.2.1. Morphological Dilation

It is one of the basic morphological operations which adds more pixels to the object boundary. Thus it enlarges[33] the boundaries of foreground pixels and effectively reduces the size of

holes present in the image. It uses a structuring element to accomplish this task. The outline of the object depends on the contour of the structuring element.

Let I be the set of coordinates in the given image and X be the set of coordinates in the structuring element. Let X*k* denote the translation of X over I so that its origin coincides with the position *k*. Then the dilation is defined as the set of all coordinates *k* such that the intersection of X*k* with I is non-empty. That is, when the origin of structuring element is superimposed on each of the background pixels, if there is at least one neighboring pixel in the structuring element that coincides with the foreground pixel, then the current pixel is converted into a foreground pixel. Else, it is left as it is.

5.2.2. Morphological Erosion

Erosion[34] is a morphological operation which does the exact opposite of dilation. Using a structuring element, it removes some pixels from the image boundaries. Let I be the set of coordinates in the input image and X be the set of coordinates in the structuring element. Let X*k* denote the translation of X over I so that its origin coincides with the position *k*. Then the erosion is defined as the set of all coordinates *k* such that X*k* is a subset of I. That is, when the origin of structuring element is superimposed on each of the foreground pixels, if all the neighboring pixel in the structuring element coincide with foreground pixels, then the current pixel is left as it is. Else, it is converted into a background pixel.

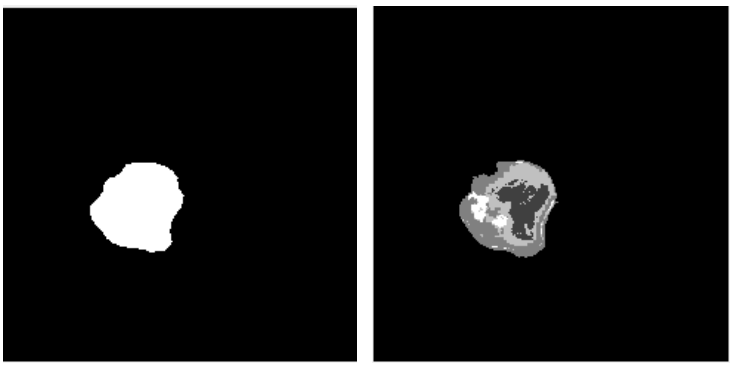

Case HGG 444: after filling holes Case HGG 444 ground truth

Fig. 5.3: Application of hole-filling algorithm

5.3. VISUALIZATION

The plotted data can be viewed in different planes such as axial, coronal and sagittal simultaneously. This provides more details to the physician while diagnosing the detected

tumor. The required slice can be specified by the user. Let the 3-dimensional volume to be viewed be I(X,Y,Z). Suppose the user wishes to view the coronal plane which gives a view along the X-Y plane. The middle slice along the Z axis whose dimension is given by DIM, is given by I(**:**,**:**,DIM/2).

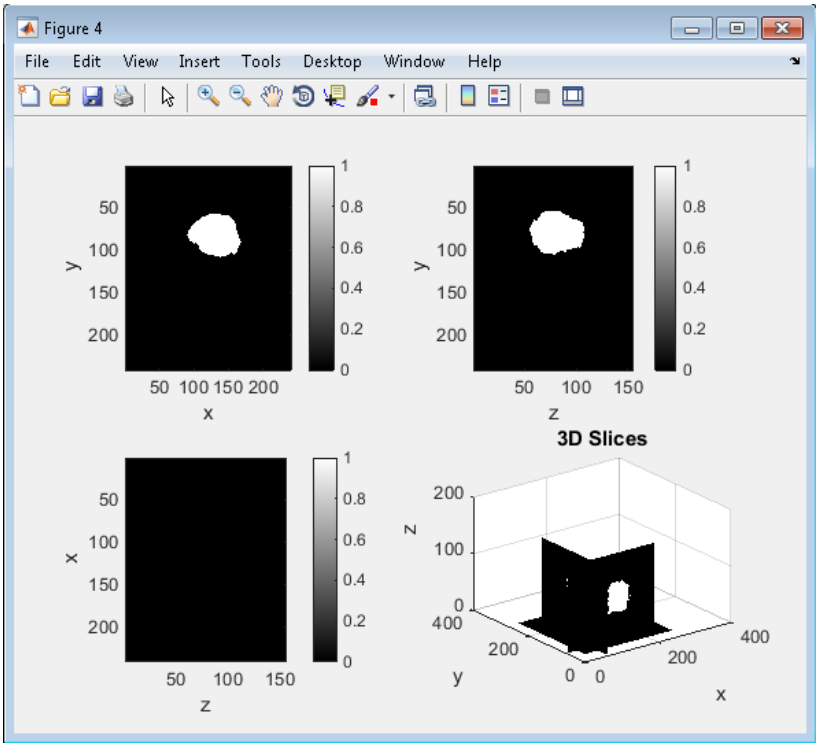

Fig. 5.4: Result as viewed in the 3 planes

CHAPTER 6

IMPLEMENTATION & VALIDATION

The dataset used for implementation is available from BRATS 2014 training data source which contains 198 cases of glioma patients. The input is a 3-dimensional volume of .mha format. This format is used to represent medical data and related to MetaImage format. It is of the dimension of 240x240x155 whose intensity values range from 0-1273. The algorithm is implemented in MATLAB computing environment on Windows Operating System. After the pre-processing step, Region split & merge method has been employed for tumor segmentation and connected component method has been used for tumor extraction. The result has been further enhanced by Region growing method. It is a 3-dimensional algorithm as the set of operations is conducted on a set of 2-D slices that forms the 3-dimensional volume. The input data-set contains T1, T1-weighted,T2 and FLAIR modalities of the MR image. We have used FLAIR modality to implement the procedure.

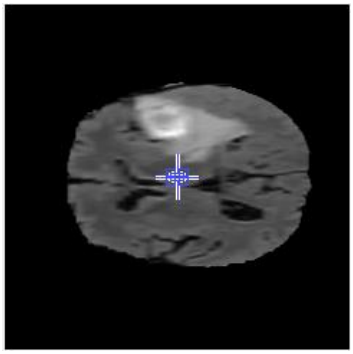

FLAIR Slice

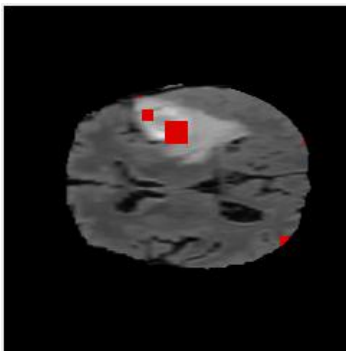

After Region Split & Merge

Result

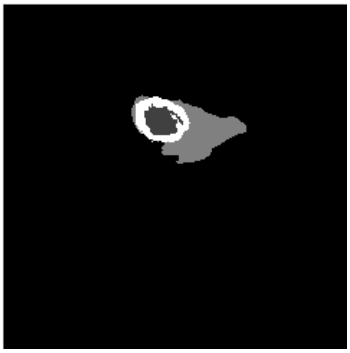

Ground truth

Fig. 6.1: Implementation on Case HGG 1

The dataset used contains the ground truth for every input, which is used to obtain the accuracy of the method employed. Dice coefficient[35] is used to measure the similarity between the segmented output and the ground truth. The minimum and maximum value of the similarity range is calculated.

$$\text{dice} = \frac{2 * \text{number of 1's (segm\_out \& ground\_truth)}}{\text{number of 1's(segm\_out)} + \text{number of 1's(ground\_truth)}} \quad (6.1)^{[35]}$$

The algorithm segmented and extracted the tumor with an accuracy ranging between 82-93%. It detected and segmented the High Grade tumors with an average accuracy of 89%. In the case of Low Grade tumors, the accuracy has decreased slightly with the average accuracy being 85%. The dice coefficient value for some representative cases has been provided in the table below:

Table 6.1: Dice coefficient value of some cases

Input data case	Dice coefficient value
HGG 1	0.943
HGG 2	0.884
HGG 153.2	0.892
HGG 162.1	0.665
HGG 474	0.939
LGG 1	0.827
LGG 8	0.926
LGG 15	0.642
LGG 254	0.932
LGG 428	0.916

The average running time on an individual slice is around 19 seconds and the average running time on the entire 3-dimansional volume with 155 slices is around 50 minutes. But this may vary as the algorithm uses a recurring function whose execution time depends on its parameters.

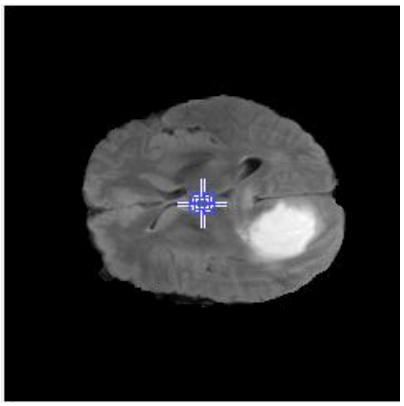

Case HGG 162.1 Flair

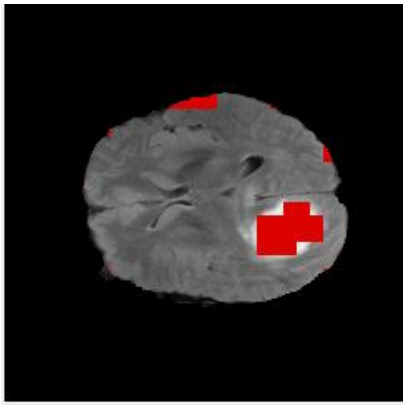

HGG 162.1 after Region Split & Merge

HGG 162.1 Result

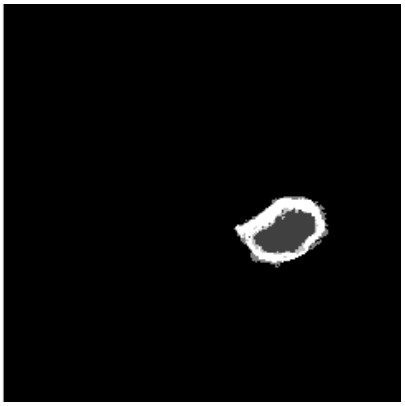

HGG 162.1 Ground Truth

Fig. 6.2: A case where the segmentation accuracy is low (Dice coefficient value – 0.665)

The accuracy of the proposed algorithm has been compared with a few of the already existing and state of the art algorithms as illustrated below:

Table 6.2: Comparison of Dice Coefficient values of different algorithms

Algorithm	**Dice Coefficient(%)**
Region Split & Merge	85(LGG),89(HGG)
Convolutional Neural Network	86(LGG),87(HGG)
Hidden Markov Model	65.6
Generative-Discriminative Hybrid Model	80

The algorithm works for a majority of input cases with a considerable accuracy. There are a few cases where the algorithm has segmented with a reduced accuracy. Another situation where the algorithm may fail segmenting the tumor is in case of multiple tumors, since the extraction step will leave out the tumor tissue.

The proposed algorithm can segment the tumors of any size, location or shape with significant accuracy. The execution time may be slightly high for some cases, which is still better compared to many of the existing algorithms. The algorithm is also automatic, hence no manual intervention is needed during the processing.

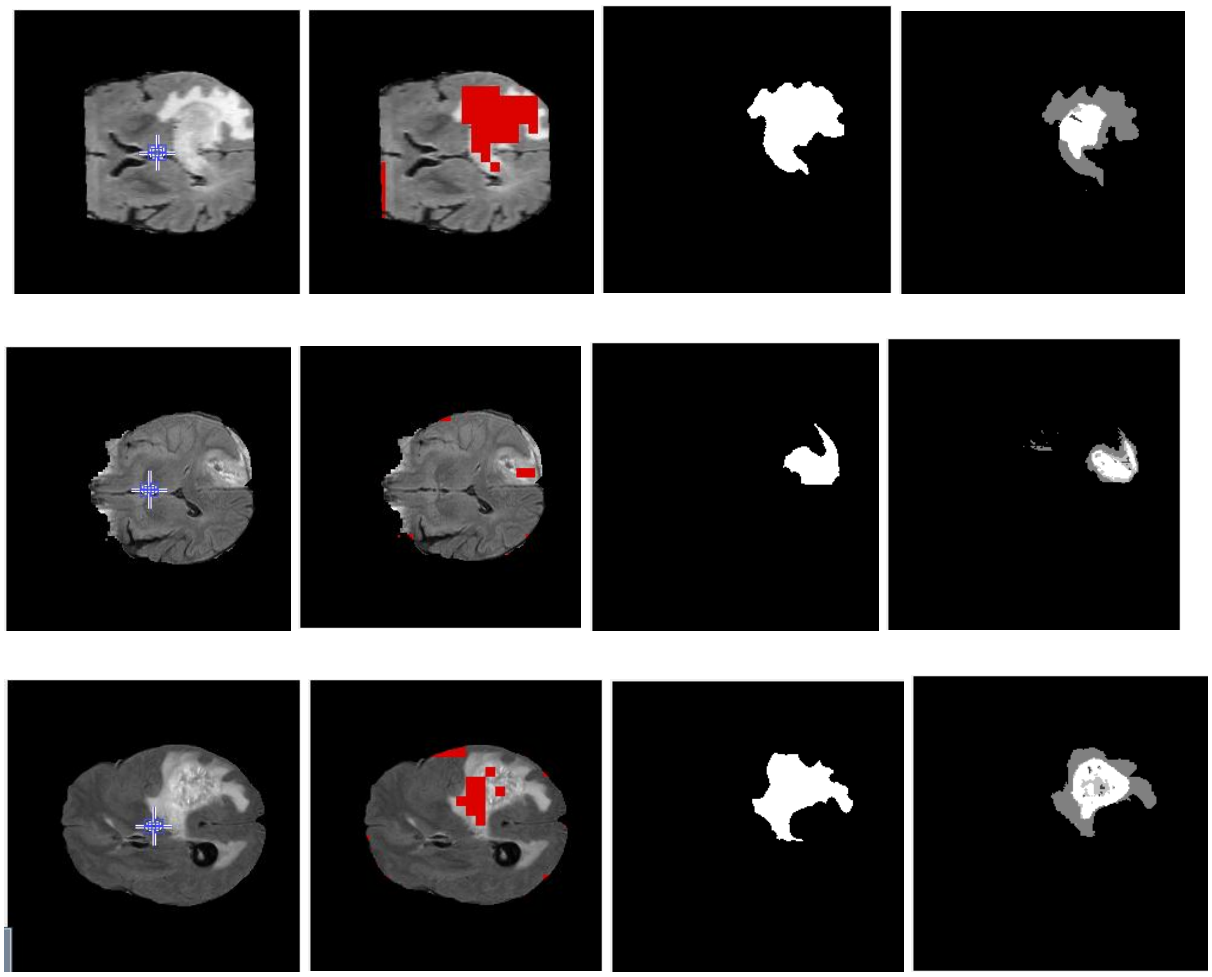

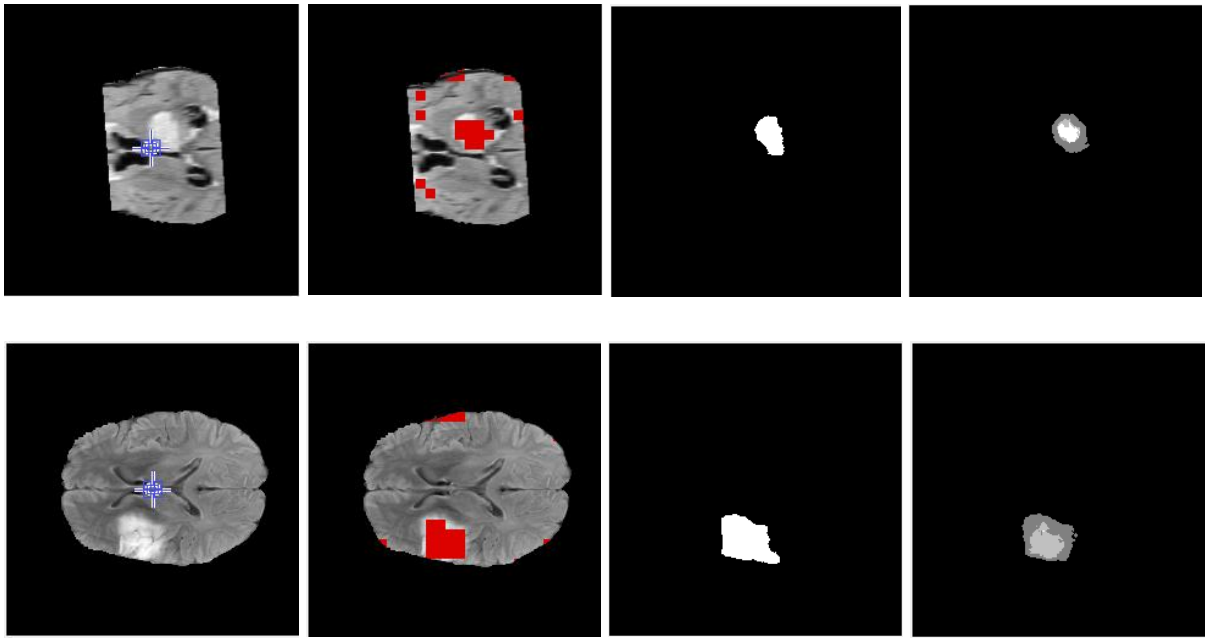

(a)Test case input (FLAIR modality) **(b)Region Split & Merge Output** **(c)Final result** **(d)Ground Truth**

Fig. 6.3: Few test cases that demonstrates the proposed algorithm (Top to bottom: HGG 3,HGG 153,HGG 474, LGG 1, LGG 428)

CHAPTER 7

CONCLUSION

In this report, we have proposed a method to detect the tumor tissues in the brain and extract them for clinical study. The algorithm combines region split & merge method and the properties of co-occurrence matrix to segment the tumor accurately. Region split & Merge method works on the principle of pixel intensity whereas Concurrence matrix provides information regarding the texture of the image. Hence this method effectively combines the image properties to achieve the goal. Apart from fixing a parameter value before the implementation of the algorithm, this method is fully automatic and hence requires no human intervention or monitoring. It can segment the tumor tissue irrespective of its size, shape and location which is a major advantage as many algorithms fail to detect the tumor that occurs close to the brain walls. The time complexity involved depends on the input data used. This is still low compared to a number of existing algorithms. The proposed method has been implemented on the dataset and the accuracy was found to be significantly high in majority of the cases. Since the dataset used contains real-life clinical cases, with further study and inclusion of all possible tumor cases, this method may be clinically applicable.

7.1. FUTURE WORK

Currently, the algorithm works with less accuracy in the case of multiple tumors. This is due to the fact that, in the case of multiple tumors, the algorithm only detects the tissue which is brighter compared to the other tumor tissues. Another aspect that can be explored is the identification of tumor components. The algorithm presently identifies only the whole tumor. Tumor components such as tumor core and edema are not identified using this algorithm. This further helps in the study of the nature of tumor and its prognosis. Hence, any future work in this direction can focus on both of these aspects.

CHAPTER 8

REFERENCE

[1] M. Prastawa, E. Bullitt, S. Ho, and G. Gerig, "A brain tumor segmentation framework based on outlier detection," Med. Image Anal. J., vol. 8, no. 3, pp. 275–283, Sep. 2004.

[2] J. J. Corso, E. Sharon, S. Dube, and S. El-Saden, "Efficient multilevel brain tumor segmentation with integrated bayesian model classification," Medical Imaging, IEEE Transactions on, vol. 27, no. 5, pp. 629–640, 2008.

[3] J. J. Thiagarajan, D. Rajan, K. N. Ramamurthy, D. Frakes, and A. Spanias, "Automated tumor segmentation using kernel sparse representations," in Proc. 12th IEEE BIBE, pp. 401–406, Nov. 2012.

[4] https://en.wikipedia.org/wiki/Brain_tumor

[5] http://www.uptodate.com/contents/primary-low-grade-glioma-in-adults-beyond-the-basics

[6] https://en.wikipedia.org/wiki/Grading_(tumors)

[7] http://www.uptodate.com/contents/primary-low-grade-glioma-in-adults-beyond-the-basics

[8] http://www.cancer.gov/types/brain/patient/adult-brain-treatment-pdq

[9] https://en.wikipedia.org/wiki/Neuroimaging

[10] http://www.fda.gov/Radiation-EmittingProducts/RadiationEmittingProductsand Procedures/MedicalImaging/MedicalX-Rays/ucm115318.htm

[11] http://science.howstuffworks.com/mri1.htm

[12] http://www.hopkinsmedicine.org/healthlibrary/test_procedures/neurological/positron_ emission_tomography_92,p07654/

[13] S. Shen, W. A. Sandham, M. H. Grant, J. Patterson, and M. F. Dempsey, "Fuzzy clustering based applications to medical image processing," in Proc. IEEE EMBS 25th Annu. Int. Conf., pp. 747–750, 2003.

[14] A. Davy, M. Havaei, D. Warde-Farley, A. Biard, L. Tran, P.M.. Jodoin, A. Courville, H. Larochelle, C. Pal, and Y. Bengio, “Brain tumor segmentation with deep neural networks”, In: MICCAI-BraTS, pp. 1–5 (2014).

[15] P. Dvorák, and B. Menze, “Structured prediction with convolutional neural networks for multimodal brain tumor segmentation”, in Proc. Multimodal Brain Tumor Image Segmentation Challenge, pp. 13–24, 2015.

[16] N. Moon, E. Bullitt, K.V. Leemput, and G. Gerig, “Model-based brain and tumor segmentation”, ICPR, Quebec, pp. 528–531, 2002.

[17] K. Xie, J. Yang, Z. Zhang, and Y. Zhu, “Semi-automated brain tumor and edema segmentation using MRI”, Eur. J. Radiol., vol. 56, pp. 12–19, 2005.

[18] M. B. Cuadra, C. Polio, A. Bardera, O. Cuisenaire, J. G. Villemure, and J.Ph. Thiran, “Atlas-based segmentation of pathological MR brain images using a model of lesion growth”, IEEE Trans. Med. Imag., Vol.23 , No.10, pp. 1301–1314, 2004.

[19] T. Taylor, N. John, P. Buendia, and M. Ryan, “Map-reduce enabled hidden Markov models for high throughput multimodal brain tumor segmentation”, Proc. Multimodal Brain Tumor Segmentation, pp. 43-46, 2013.

[20] R. Meier1 , S. Bauer , J. Slotboom , R. Wiest , and M. Reyes, “ A Hybrid Model for Multimodal Brain Tumor Segmentation”.Proc. BRATS MICCAI 2013, pp. 31–36, 2013.

[21] S. Bakas, K. Zeng, A. Sotiras, S. Rathore, H. Akbari, B. Gaonkar, M. Rozycki, S. Pati, and C. Davatzikos, “Segmentation of Gliomas in Multimodal Magnetic Resonance Imaging Volumes Based on a Hybrid Generative-Discriminative Framework”, Proc. BRATS MICCAI 2015, pp. 5-12, 2015.

[22] F.P. Fischmeister, I. Höllinger, N. Klinger, A. Geissler, M.C. Wurnig, and E. Matt, “The benefits of skull stripping in the normalization of clinical fMRI data”, Neuroimage Clinical 2013, vol. 3, pp. 369–380, 2013

[23] P.Kalavathi, and V. B. Surya Prasath, “Methods on Skull Stripping of MRI Head Scan Images—a Review”, Journal of Digital Imaging, pp. 1-15, 2015.

[24] R. Jain, R. Kasturi, and B. Schunck, “Machine Vision”, McGraw-Hill, Inc., ISBN 0-07-032018-7, 1995

[25] R.M. Haralick, K. Shanmugan, and I. Dinstein, "Textural Features for Image Classification", IEEE Transactions on Systems, Man, and Cybernetics, Vol. SMC-3, 1973, pp. 610-621

[26] http://in.mathworks.com/help/images/ref/graycoprops.html

[27] L. Di Stefano and A. Bulgarelli , "A simple and efficient connected components labeling algorithm", Proc. International Conference on Image Analysis and Processing, pp.322 -327, 1999.

[28] Electronic Supplementary Material (ESI) for Biomaterials Science, The Royal Society of Chemistry 2014, 2014.

[29] S. Kamdi, "Image Segmentation and Region Growing Algorithm", International Journal of Computer Technology and Electronics Engineering (IJCTEE), Vol 2 Issue no.1, October 2011

[30] https://en.wikipedia.org/wiki/Centroid

[31] S. Gupta, and P. Kumar, "Automated Region Growing Approach for Brain Tumor Segmentation in 3D MR Images", International Journal of Information Processing, vol. 7, no. 4, pp. 1-10, 2013.

[32] P. Soille, Morphological Image Analysis: Principles and Applications, Springer, 1999, pp. 164-165.

[33] http://homepages.inf.ed.ac.uk/rbf/HIPR2/dilate.htm

[34] http://homepages.inf.ed.ac.uk/rbf/HIPR2/erode.htm

[35] S. Warfield, K. Zou, and W. Wells, "Simultaneous truth and performance level estimation (STAPLE): an algorithm for the validation of image segmentation", IEEE Trans. Med. Imag., vol. 23, pp. 903–921, 2004.

[36] http://www.phytoscience.ca/articles/Cancer%20-%20Brain%20Tumor.html

[37] http://www.med.wayne.edu/diagRadiology/Anatomy_Modules/brain/brain.html